nature neuroscience

NGL family PSD-95–interacting adhesion molecules regulate excitatory synapse formation

Seho Kim[1], Alain Burette[2], Hye Sun Chung[3], Seok-Kyu Kwon[1], Jooyeon Woo[1], Hyun Woo Lee[1], Karam Kim[1], Hyun Kim[3], Richard J Weinberg[2,4] & Eunjoon Kim[1]

Synaptic cell adhesion molecules (CAMs) regulate synapse formation through their trans-synaptic and heterophilic adhesion. Here we show that postsynaptic netrin-G ligand (NGL) CAMs associate with netrin-G CAMs in an isoform-specific manner and, through their cytosolic tail, with the abundant postsynaptic scaffold postsynaptic density–95 (PSD-95). Overexpression of NGL-2 in cultured rat neurons increased the number of PSD-95–positive dendritic protrusions. NGL-2 located on heterologous cells or beads induced functional presynaptic differentiation in contacting neurites. Direct aggregation of NGL-2 on the surface membrane of dendrites induced the clustering of excitatory postsynaptic proteins. Competitive inhibition by soluble NGL-2 reduced the number of excitatory synapses. NGL-2 knockdown reduced excitatory, but not inhibitory, synapse numbers and currents. These results suggest that NGL regulates the formation of excitatory synapses.

Precise control of synaptogenesis is essential for neurons to establish correct connectivity. CAMs promote synapse formation through trans-synaptic adhesions[1–8]. The ideal synaptogenic CAM would concentrate at synapses and mediate a heterophilic adhesion between axons and dendrites to avoid inappropriate homophilic connections. Moreover, its cytosolic region would interact with scaffolding proteins to couple adhesion events with the recruitment of synaptic proteins.

Among the neuronal CAMs previously identified[3,4,9–12], only neuroligin exhibits all these ideal characteristics[11,13–18]. Postsynaptic neuroligin associates with presynaptic neurexin[11], inducing bidirectional synaptic differentiation[15–21]. C termini of both molecules bind to cytosolic PDZ (postsynaptic density-95/discs large/zona occludens-1) domain–containing scaffolds; neuroligin associates with PSD-95 (refs. 14,15), and neurexin with CASK and Mint (refs. 22,23). Alternative splicing of both neurexin and neuroligin regulates their adhesion and synapse induction[13,24–28]. Neuroligin 1 and neuroligin 2 mainly distribute to excitatory and inhibitory synapses, respectively[16,17,21,29,30], and regulate their formation[16,17,19,21,31,32]. These results implicate the neurexin-neuroligin complex in synapse formation, but the huge diversity of neuronal synapses in the brain suggests the presence of new pairs of adhesion receptors and ligands that are heterophilic and synaptogenic.

Netrin-G/laminet is a family of CAMs (netrin-G1/laminet-1 and netrin-G2/laminet-2) that are preferentially expressed in the central nervous system[33–35]. Netrin-G is similar in its structure to the netrin/UNC-6 family of axon guidance molecules but unique in that it does not bind to known netrin receptors such as UNC-5H and DCC/UNC-40 and is linked to the plasma membrane through a glycosyl phosphatidylinositol (GPI) anchor. mRNAs of netrin-G1 and netrin-G2 show largely nonoverlapping distribution patterns in the brain[33–35], suggesting that they contribute to the formation of distinct neural connections. Recently, a new ligand of netrin-G1, termed NGL-1, was reported[36]. Disrupting the interaction between netrin-G1 and NGL-1 by soluble NGL-1 inhibits the growth of embryonic thalamic axons[36], suggesting that the netrin-G1–NGL-1 interaction is important for the development of thalamic axons during embryonic stages. The expression of both netrin-G1 and netrin-G2 in the brain continues into postnatal and even adult stages[33–35], but little is known about their roles in the later stages of brain development.

In the present study, we show that netrin-G and NGL family proteins bind in an isoform-specific manner and that the C terminus of NGL associates with PSD-95. The results from various experiments, including neuron-fibroblast coculture, bead-induced synaptic differentiation, competition by soluble proteins, overexpression and siRNA knockdown, suggest that NGL is involved in the formation of excitatory, but not inhibitory, synapses.

RESULTS

Interaction of NGL with PSD-95

Ultrastructural studies demonstrate that PSD-95 concentrates near the postsynaptic membrane[37], in an ideal position to associate with synaptic CAMs. Our yeast two-hybrid screen of mouse cDNAs with the PDZ domains of PSD-95 identified a CAM. Because a related protein in the same family has been named NGL-1 (ref. 36), we followed this nomenclature and designated our protein NGL-2 and the third member in the database NGL-3. NGLs share a common domain

[1]National Creative Research Initiative Center for Synaptogenesis and Department of Biological Sciences, Korea Advanced Institute of Science and Technology, Daejeon 305-701, Korea. [2]Department of Cell and Developmental Biology, University of North Carolina, Chapel Hill, North Carolina 27599, USA. [3]Department of Anatomy and Division of Brain Korea 21, Biomedical Science, College of Medicine, Korea University, Seoul 136-705, Korea. [4]Neuroscience Center, University of North Carolina, Chapel Hill, North Carolina 27599, USA. Correspondence should be addressed to E.K. (kime@kaist.ac.kr).

Received 30 June; accepted 14 August; published online 17 September 2006; doi:10.1038/nn1763

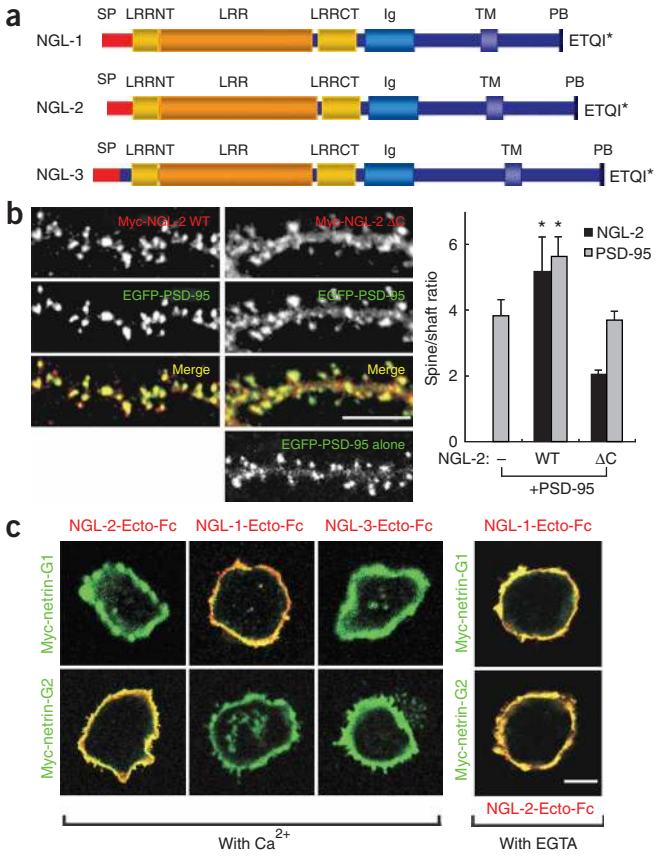

Figure 1 NGL interacts with PSD-95 through its C terminus and with netrin-G CAMs through its ectodomain in an isoform-specific manner. (**a**) Domain structure of NGL. SP, signal peptide; LRR, leucine-rich repeat; LRRNT, LRR N-terminal domain; LRRCT, LRR C-terminal domain; Ig, immunoglobulin domain; TM, transmembrane domain; PB, PDZ domain–binding motif; ETQI*, the last four aa residues of NGL. (**b**) NGL-2 and PSD-95 are interdependent for spine localization. In cultured hippocampal neurons (days *in vitro*, DIV, 17–19), wild-type (WT) NGL-2 showed a higher degree of spine localization (relative intensity of NGL-2 in spine versus dendritic shaft; $n = 20$ neurons; 30 ratios per neuron) compared to NGL-2 ΔC lacking the last three residues. Note that PSD-95 coexpressed with NGL-2 wild type has an increased spine localization compared with PSD-95 expressed alone or coexpressed with NGL-2 ΔC. Data represent mean ± s.e.m. (**c**) Isoform-specific and calcium-independent adhesion between netrin-G and NGL family proteins. The ectodomain of NGL-2 fused to the Fc domain of immunoglobulin (NGL-2-Ecto–Fc), and NGL-1-Ecto–Fc selectively bound Myc–netrin-G2a (a splice variant of netrin-G2) and Myc–netrin-G1c (a splice variant of netrin-G1), respectively, in HEK293T cells. NGL-3 did not bind to either netrin-G1 or netrin-G2. Fc alone, negative control. Chelation of calcium with 10 mM EGTA did not affect the association between NGL-2 and netrin-G2, or NGL-1 and netrin-G1. Scale bar in **b**,**c**: 10 μm.

structure: leucine-rich repeats (LRRs) flanked by the LRR N- and C-terminal domains and an immunoglobulin domain in the extracellular side, a transmembrane domain and a C-terminal PDZ domain–binding motif (**Fig. 1a** and **Supplementary Fig. 1** online).

NGL C termini interacted with the first two PDZ domains of PSD-95 family proteins in a yeast two-hybrid, pull-down, *in vitro* coimmunoprecipitation, and in coclustering assays (**Supplementary Fig. 2** online). In the brain, NGL-2 formed a complex with PSD-95 and NMDA receptors (NR1 and NR2B subunits) but not with AMPA receptors (GluR1 and GluR2; **Supplementary Fig. 2**). In transfected neurons, wild-type NGL-2 exhibited ~2.5 times higher spine localization than NGL-2 ΔC that lacks the PSD-95–interacting C terminus (**Fig. 1b**). In contrast, PSD-95 coexpressed with NGL-2 wild type showed higher spine localization (~50%) compared with PSD-95 alone or PSD-95 coexpressed with NGL-2 ΔC (**Fig. 1b**), suggesting that NGL-2 and PSD-95 are interdependent for synaptic localization.

Characteristics of the NGL–netrin-G interaction

Because NGL and netrin-G families have three and two isoforms, respectively[33–35], we tested for isoform-specific adhesions. The ectodomain of NGL-2 fused to the immunoglobulin Fc domain (NGL-2-Ecto–Fc selectively bound netrin-G2 expressed in HEK293T cells, but not netrin-G1 (**Fig. 1c**). NGL-1-Ecto–Fc bound netrin-G1, as previously reported[36], but not netrin-G2. NGL-3-Ecto–Fc did not interact with either netrin-G1 or netrin-G2. Calcium depletion did not affect NGL binding to netrin-G (**Fig. 1c**). These results suggest that the adhesion between NGL and netrin-G family proteins is isoform specific and calcium independent.

It is not known whether NGL and netrin-G mediate cell adhesion. L cells transiently expressing NGL-1 and NGL-2 selectively aggregated with cells expressing netrin-G1 and netrin-G2, respectively (**Supplementary Fig. 3** online), suggesting that the association between NGL and netrin-G mediates cell adhesion in an isoform-specific manner.

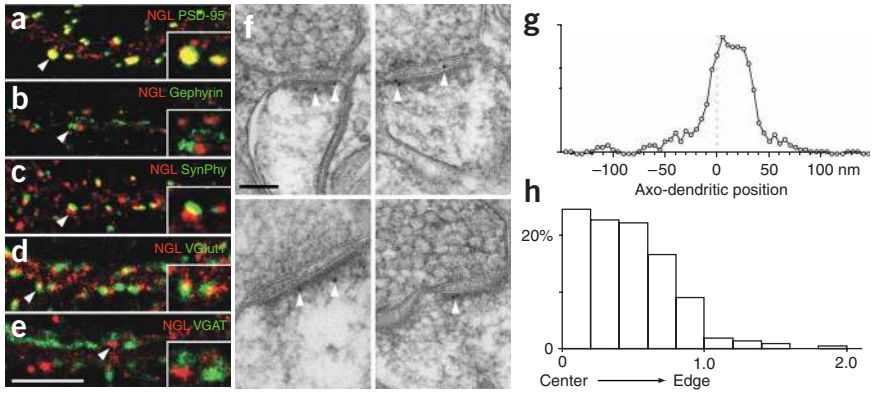

Figure 2 NGL localizes to the postsynaptic side of excitatory synapses. (**a**–**e**) Selective localization of NGL at excitatory synapses. Cultured hippocampal neurons (DIV 21) were doubly labeled for NGL and the indicated subcellular markers. Enlarged regions are indicated by arrowheads. Gephyrin, inhibitory postsynaptic marker; SynPhy, synaptophysin; VGlut1, excitatory presynaptic marker; VGAT, inhibitory presynaptic marker. Scale bar, 10 μm. (**f**) Ultrastructural localization of NGL in the postsynaptic density (examples from the CA1 region of hippocampus; 10 nm gold particles). Scale bar, 100 nm. (**g**) NGL immunogold particles were concentrated on the postsynaptic side of the synapse, within ~30 nm from the plasma membrane. Abscissa represents the distance from the center of each gold particle to the outer leaflet of the postsynaptic membrane (0 nm, dashed line); the ordinate is the labeling density (arbitrary units); data smoothed with three-point weighted running average. (**h**) NGL immunogold particles concentrate centrally along the lateral axis of the synapse. Lateral position is normalized; the center of the active zone corresponds to 0, the edge to 1.0.

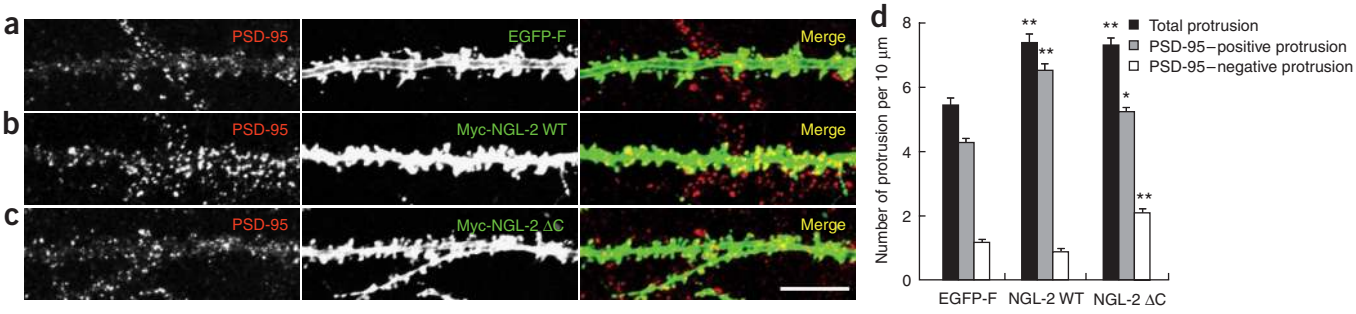

Figure 3 Overexpression of NGL-2 increases the number of PSD-95–positive dendritic protrusions through both PSD-95–dependent and PSD-95–independent mechanisms. (**a**–**c**) Cultured hippocampal neurons were transfected at DIV 10 with farnesylated EGFP (EGFP-F, **a**), Myc–NGL-2 WT (**b**) or Myc–NGL-2 ΔC (**c**), and immunostained at DIV 17 for PSD-95 and Myc or EGFP. Scale bar, 10 μm. (**d**) NGL-2 expression increased the number of total and PSD-95–positive dendritic protrusions. Note that NGL-2 ΔC also increased the total number of dendritic protrusions; however, an increase in the number of PSD-95–negative protrusions occurred at the expense of PSD-95–positive protrusions. Mean ± s.e.m. $n = 54$ cells for NGL-2, 27 for EGFP-F alone and 45 for NGL-2 ΔC. $^*P < 0.001$ and $^{**}P < 0.0001$ (Student's *t*-test).

Expression patterns of NGL mRNAs and proteins

NGL-2 and *NGL-3* mRNAs are mainly expressed in the brain (**Supplementary Fig. 4** online), as previously reported for *NGL-1* (ref. 36). *NGL-2* mRNAs concentrated in the olfactory bulb, cortex, hippocampus and cerebellum in adult rat brain (6 weeks); *NGL-1* mRNA in the cortex, hippocampus and striatum; and *NGL-3* was widespread throughout the brain (**Supplementary Fig. 4**). Consistent with the adhesion-mediated synaptogenic role suggested below, *netrin-G* and *NGL* mRNAs were expressed in regions of the early postnatal brain (postnatal day, P, 14), between which synaptogenesis can occur. These include expression of *netrin-G2* and *NGL-2* mRNA in hippocampal CA3 and CA1 (a target for CA3 pyramidal neurons), respectively, and expression of *netrin-G1* and *NGL-1* mRNA in the thalamus and cortex (a target area for thalamic innervation), respectively (**Supplementary Fig. 4**), similar to the results from mouse brain (P20–21; refs. 33,35). NGL proteins (~100 kDa), revealed by the NGL antibody that recognizes all three NGL isoforms, were brain specific, widely expressed in brain regions, detected in synaptic fractions, enriched in PSD fractions and sharply upregulated during postnatal brain development (**Supplementary Fig. 4**). N-glycosidase F reduced the molecular weight of NGL (**Supplementary Fig. 4**), suggesting that NGL is N-glycosylated.

NGL in cultured neurons was detected at synaptic sites, colocalizing with synaptophysin (presynaptic marker), vesicular glutamate transporter 1 (VGlut1, excitatory presynaptic marker) and PSD-95 (76.3% of NGL clusters were PSD-95 positive, $n = 871$), but not with vesicular GABA transporter (VGAT, inhibitory presynaptic marker) or gephyrin (inhibitory postsynaptic marker) (**Fig. 2a**–**e**). In brain sections, punctate NGL clusters colocalized with synaptophysin (69.2%, $n = 423$) and were frequently associated with the tips of dendritic spines (**Supplementary Fig. 5** online). Ultrastructurally, NGL was mainly postsynaptic, concentrating within ~30 nm of the postsynaptic membrane, and was more abundant in the center of the synapse than at the periphery (**Fig. 2f**–**h**).

NGL-2 overexpression promotes dendritic protrusions

To investigate the possible involvement of NGL in synapse formation, we first examined the effects of NGL-2 overexpression in cultured hippocampal neurons. We used NGL-2 rather than NGL-1 because both NGL-2 and its binding partner netrin-G2 are expressed in hippocampal neurons, allowing the study of their involvement in synapse formation in a single well-characterized preparation. NGL-2 overexpression in neurons increased the total and PSD-95–positive, but

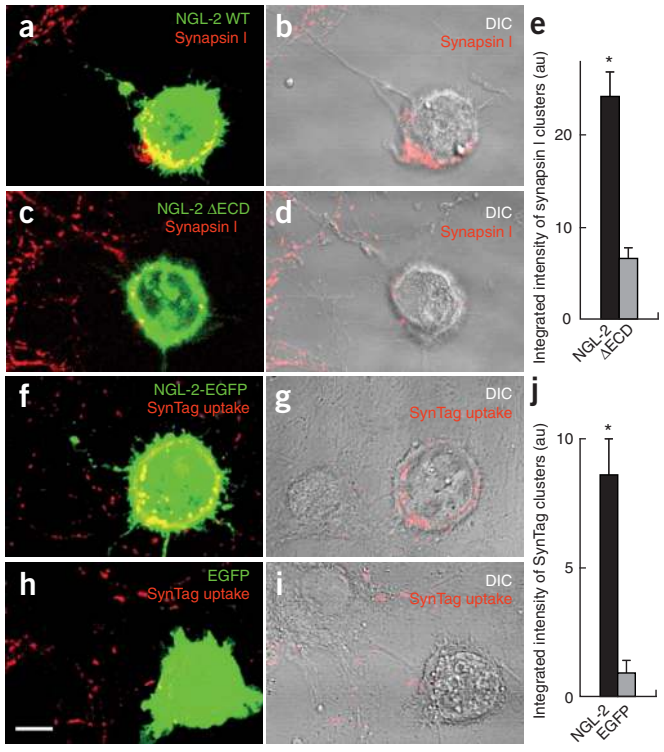

Figure 4 NGL-2 expression in heterologous cells induces functional presynaptic differentiation in contacting neurites. (**a**–**d**) HEK293T cells expressing Myc–NGL-2 (**a**,**b**) or NGL-2 ΔECD (**c**,**d**; control), were cocultured with hippocampal neurons (DIV 9–12) and stained for Myc and synapsin I. Scale bar, 10 μm. (**e**) Quantitation of the integrated intensity of NGL-2–induced synapsin I clusters. Mean ± s.e.m. $n = 28$ for NGL-2 wild type and $n = 37$ for NGL-2 ΔECD. $^*P < 0.0001$ (Student's *t*-test). au, arbitrary unit. (**f**–**i**) HEK293T cells expressing NGL-2-EGFP (**f**,**g**) or EGFP alone (**h**,**i**; control) were cocultured with hippocampal neurons (DIV 9–12) and stained with EGFP and synaptotagmin (SynTag) luminal domain antibodies. Scale bar, 10 μm. (**j**) Quantitation of the integrated intensity of NGL-2–induced synaptotagmin clusters. Mean ± s.e.m. $n = 27$ for NGL-2–EGFP and 24 for EGFP. $^*P < 0.0001$ (Student's *t*-test).

not PSD-95–negative, number of dendritic protrusions (**Fig. 3a**,**b**). A large fraction of the PSD-95–positive dendritic protrusions (~89%) was positive for the presynaptic marker synapsin I.

NGL-2 ΔC similarly increased the total number of dendritic protrusions but increased PSD-95–negative dendritic protrusions at the expense of PSD-95–positive ones (**Fig. 3c**,**d**). This suggests that NGL-2 promotes the formation of PSD-95–positive dendritic protrusions through two distinct mechanisms: C terminus–dependent PSD-95 clustering and C terminus–independent formation of dendritic protrusions.

NGL-2 in HEK293 cells induces presynaptic differentiation

To test whether NGL induces presynaptic differentiation, we performed a neuron-fibroblast coculture assay, previously used to demonstrate the synaptogenic activity of neuroligin, β-neurexin and SynCAM (refs. 9,17,18). NGL-2–expressing HEK293T cells induced the clustering of synapsin I in contacting neurites (**Fig. 4a**,**b**). In contrast, an NGL-2 mutant lacking the extracellular domain (NGL-2 ΔECD) showed a substantially lower synapsin I clustering, as quantified by the integrated intensity of synapsin I on HEK293T cells (**Fig. 4c–e**). The NGL-2–induced presynaptic specializations were functional, as indicated by the uptake of synaptotagmin luminal domain antibodies[38], whereas control cells induced minimal antibody uptake (**Fig. 4f–j**). These results suggest that NGL-2 induces functional presynaptic differentiation through a trans-synaptic adhesion.

Beads bearing NGL-2 induce presynaptic differentiation

The presynaptic differentiation induced by NGL-2–expressing heterologous cells may be aided by other membrane proteins on the cells. However, beads bearing NGL-2-Ecto–Fc induced the clustering of synaptophysin and VGlut1, but not VGAT or PSD-95, in contacting neurites (**Fig. 5a–d**). In addition, the beads induced the clustering of exogenous netrin-G2 (**Fig. 5e**), a netrin-G isoform highly expressed in the hippocampus[34,35], which distributes to axons when expressed in cultured neurons (**Supplementary Fig. 6** online). The bead-induced presynaptic specializations were functional, as indicated by the uptake of synaptotagmin luminal domain antibodies (**Fig. 5f**).

The fluorescence intensity associated with the bead aggregates normalized to nearby regions was 4.29 ± 0.60 (n = 80 bead aggregates) for synaptophysin, 4.24 ± 0.47 (n = 158) for VGlut1, 14.48 ± 2.07 (n = 142) for netrin-G2 and 4.74 ± 0.35 (n = 82) for synaptotagmin, but 1.08 ± 0.17 (n = 105) for VGAT and 0.95 ± 0.08 (n = 138) for PSD-95. These results collectively suggest that NGL-2 is sufficient to induce excitatory presynaptic differentiation through a trans-synaptic adhesion.

Direct NGL-2 aggregation clusters postsynaptic proteins

If NGL-2 is an important synaptogenic molecule, its direct aggregation on the dendritic surface should induce clustering of postsynaptic proteins. Therefore, neurons expressing a form of NGL-2 in which EGFP was tagged to the N terminus were incubated with EGFP antibody–coated beads. The beads induced robust NGL-2 aggregation at sites of bead contact on dendrites (**Fig. 6a**) and coclustering of PSD-95 and other postsynaptic receptors and scaffolding proteins including NR2A (NMDA receptors), GKAP and Shank (fluorescent intensities normalized to nearby regions were 4.36 ± 0.55, n = 27; 3.30 ± 0.39, n = 61; 4.24 ± 0.37, n = 53; and 2.86 ± 0.20, n = 25, respectively; **Fig. 6a–d**).

The postsynaptic protein clusters induced by NGL-2 aggregation were not associated with synapsin I (**Fig. 6a–d**), suggesting that they were not induced by interneuronal synapses. The beads did not induce coclustering of GluR2 (surface) and gephyrin (0.86 ± 0.13, n = 65; 0.94 ± 0.17, n = 35, respectively; **Fig. 6e**,**f**). These results indicate that NGL-2 is sufficient to induce selective clustering of excitatory postsynaptic proteins.

Soluble NGL-2 reduces the number of excitatory synapses

We competitively inhibited NGL-2 adhesions by incubating cultured neurons with soluble NGL-2 (NGL-2-Ecto–Fc). This substantially reduced the number of total and synaptophysin-positive, but not synaptophysin-negative, dendritic protrusions—by ~20% (**Fig. 7a**,**b**)—suggesting that the adhesion between netrin-G2 and NGL-2 is required for the maintenance of excitatory synapses.

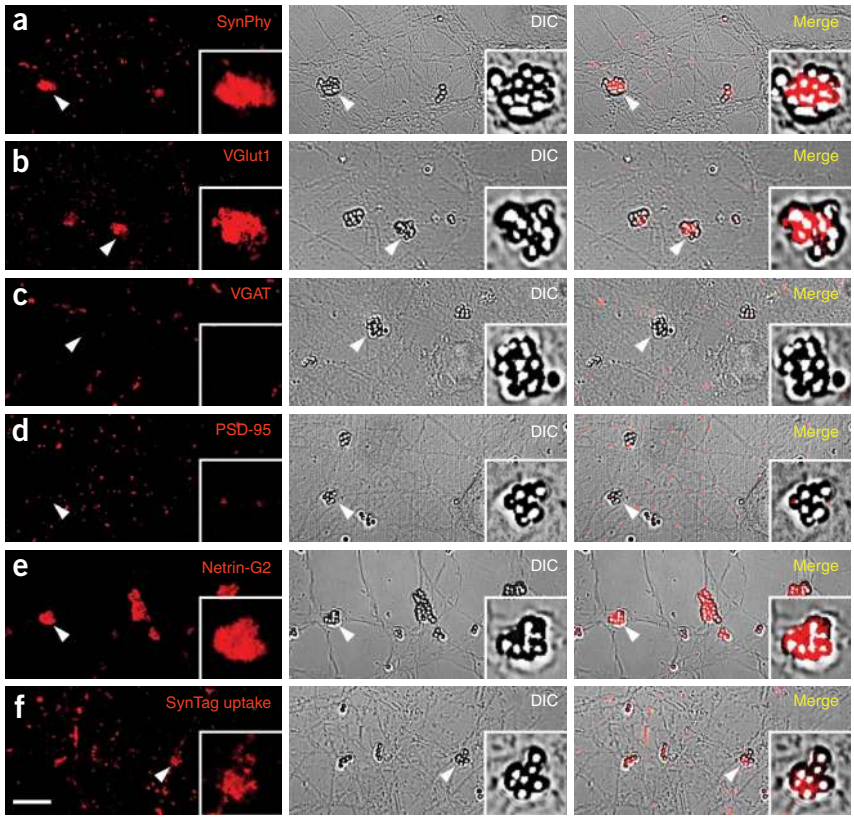

Figure 5 Beads bearing the ectodomain of NGL-2 induce functional excitatory presynaptic differentiation in contacting neurites. (**a**–**f**) Cultured hippocampal neurons, untransfected (DIV 12; **a**–**d**,**f**) or transfected with netrin-G2 (DIV 9–12; **e**), were incubated with beads coated with NGL-2-Ecto–Fc (DIV 12–13). The beads induced the clustering of synaptophysin (**a**), VGlut1 (**b**) and netrin-G2 (**e**), but not that of VGAT (**c**) and PSD-95 (**d**), in contacting neurites. In addition, the beads induced the uptake of synaptotagmin (luminal domain) antibodies (**f**). Beads were visualized by differential interference contrast (DIC) imaging. Enlarged beads are indicated by arrowheads. Scale bar, 10 μm.

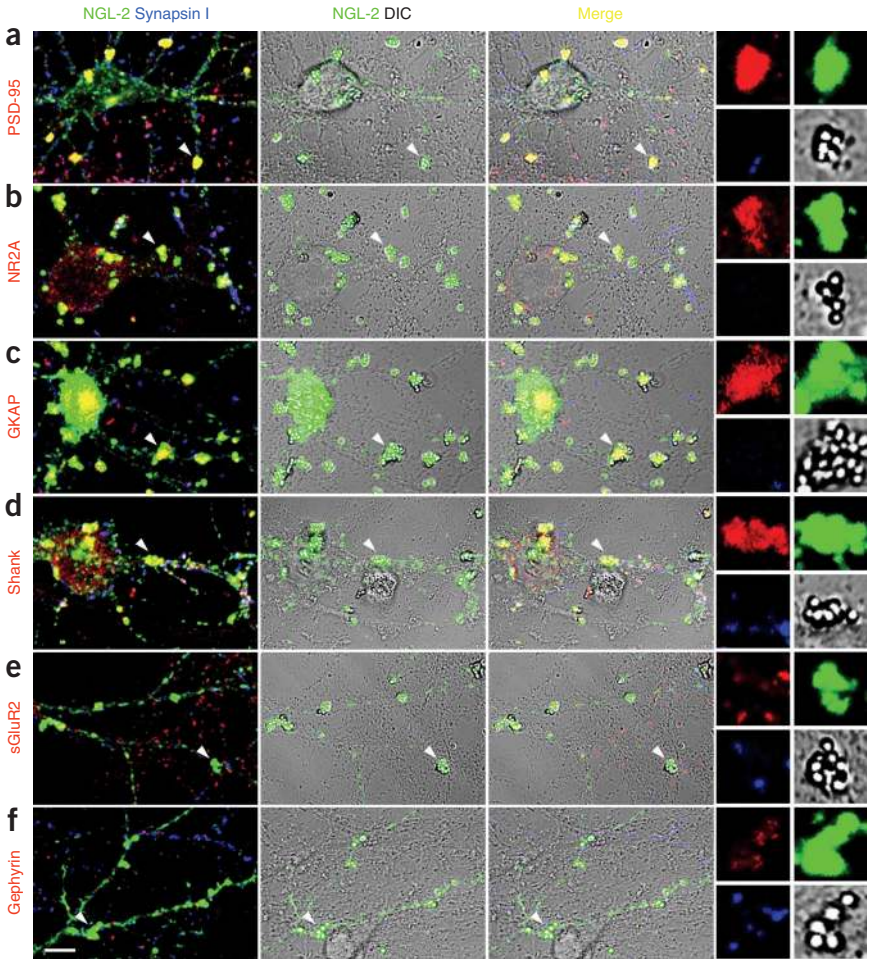

Figure 6 Direct aggregation of NGL-2 on the dendritic surface induces clustering of excitatory postsynaptic proteins. (**a**–**f**) Cultured hippocampal neurons expressing NGL-2 tagged with EGFP at the N terminus (DIV 14–16) were incubated with EGFP antibody–coated beads and visualized at DIV 17 by triple immunofluorescence staining for EGFP (NGL-2), synapsin I and PSD-95 (**a**) or the indicated synaptic proteins (**b**–**f**). NR2A, the NR2A subunit of NMDA glutamate receptors; GluR2, the GluR2 subunit of AMPA glutamate receptors. Scale bar, 10 μm. Enlarged beads are indicated by arrowheads.

NGL-2 knockdown reduces the number of excitatory synapses

Finally, NGL-2 siRNA knockdown in cultured hippocampal neurons significantly reduced the number of excitatory synapses (VGlut1-positive PSD-95 clusters; **Fig. 8a**,**b** and **Supplementary Fig. 7** online), an effect rescued by coexpression of siRNA-resistant NGL-2 (**Fig. 8c**,**d** and **Supplementary Fig. 7**). In contrast, NGL-2 knockdown did not affect inhibitory synapses (VGAT-positive gephyrin clusters; **Fig. 8e**–**g**).

Functionally, NGL-2 knockdown reduced the frequency, but not the amplitude, of miniature excitatory postsynaptic currents (mEPSCs) (**Fig. 8h**–**j**), whereas there was no change in the frequency or amplitude of miniature inhibitory postsynaptic currents (mIPSCs) (**Fig. 8k**–**m**). These results suggest that NGL-2 is required for the morphological and functional maintenance of excitatory, but not inhibitory, synapses.

DISCUSSION

Role of the adhesion between netrin-G and NGL

NGL-2 expressed on fibroblasts or beads promotes functional presynaptic differentiation in contacting axons. Direct aggregation of NGL-2 on the surface membrane of dendrites induces the clustering of excitatory postsynaptic proteins. Soluble NGL-2 and NGL-2 knockdown reduces the number of excitatory synapses. Taken together, these results suggest that the netrin-G–NGL adhesion promotes excitatory synapse formation.

How might netrin-G2, a GPI-anchored protein without the intracellular region[33], promote presynaptic differentiation? Netrin-G2 may cluster into lipid rafts and directly associate with and activate related signaling molecules[39]. However, it should be noted that direct bead aggregation of netrin-G2 on the axonal surface did not induce presynaptic differentiation, and netrin-G2–expressing HEK293T cells did not induce postsynaptic differentiation in contacting dendrites (S.K. and E.K., unpublished data). This suggests that netrin-G2 may require as yet unknown coreceptors for presynaptic differentiation. A previous study similarly concluded that netrin-G1 may only be a part of the NGL-1 receptor, because soluble NGL-1, but not soluble netrin-G1, is sufficient to disrupt the growth of thalamic neurons[36]. Identification of additional NGL binding partners will be an important direction for future studies.

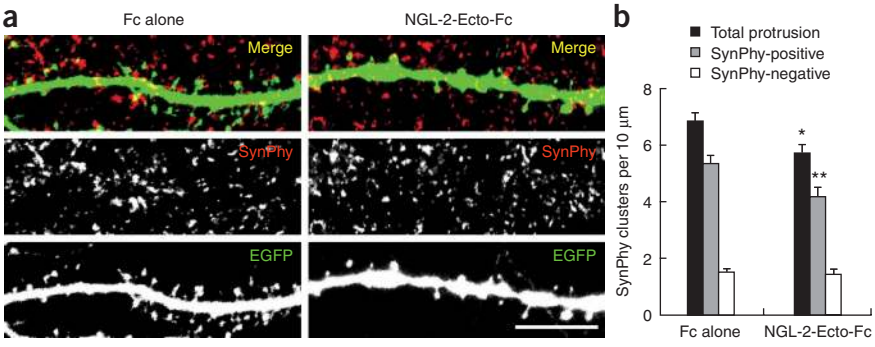

Figure 7 Soluble NGL-2 fusion proteins reduce the number of excitatory synapses. (**a**) Cultured hippocampal neurons transfected with pEGFP-C1 (for visualization of dendritic protrusions; DIV 12–15) were incubated with NGL-2-Ecto–Fc fusion proteins, or Fc alone (control), for 3 d (DIV 15–18) and stained for EGFP and synaptophysin. Scale bar, 10 μm. (**b**) NGL-2-Ecto–Fc reduced the number of total and synaptophysin-positive, but not synaptophysin-negative, dendritic protrusions. Mean ± s.e.m. $n = 24$ cells for Fc alone and 33 for NGL-2-Ecto–Fc. $^{*}P < 0.05$, $^{**}P < 0.01$ (Student's *t*-test).

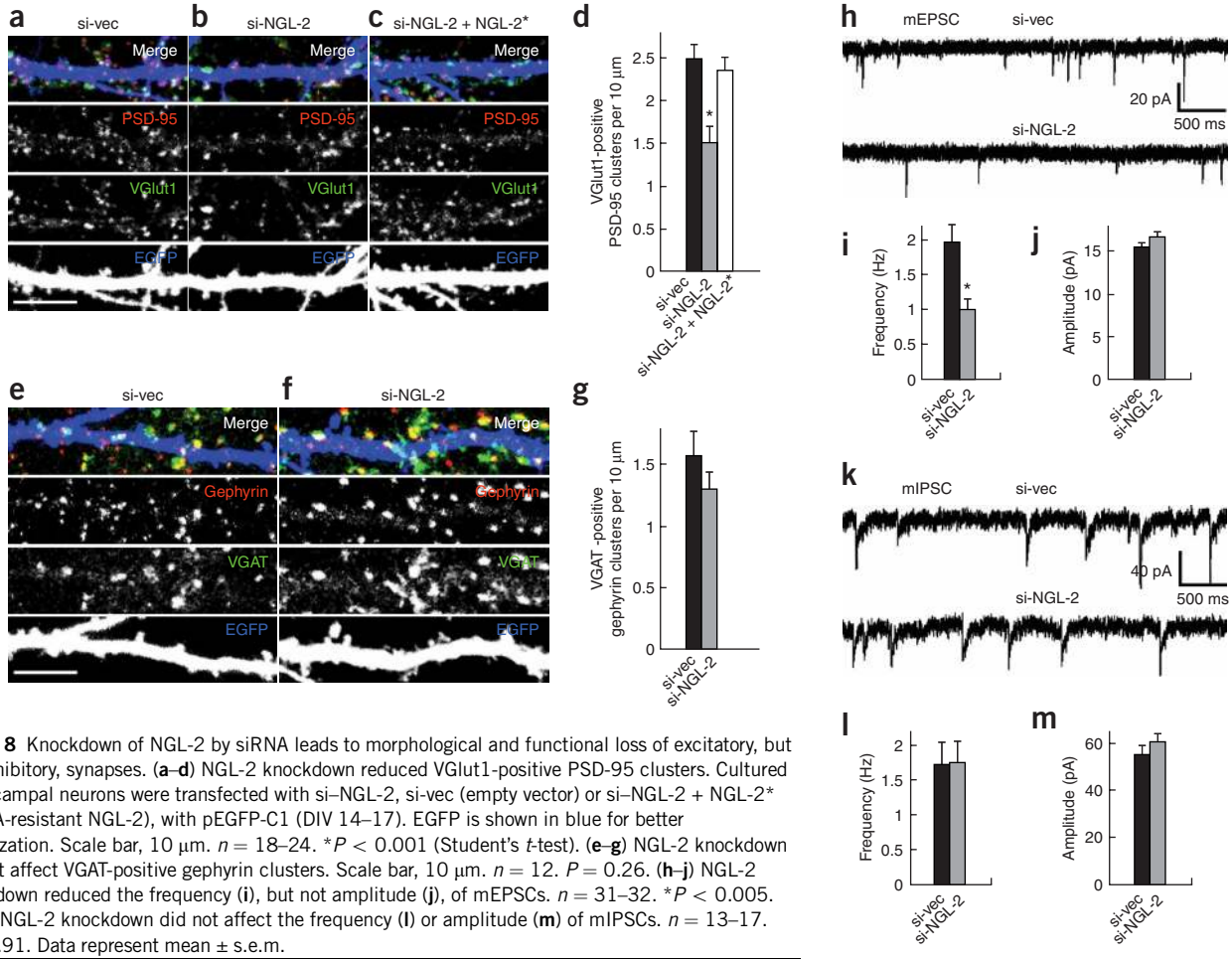

Figure 8 Knockdown of NGL-2 by siRNA leads to morphological and functional loss of excitatory, but not inhibitory, synapses. (**a**–**d**) NGL-2 knockdown reduced VGlut1-positive PSD-95 clusters. Cultured hippocampal neurons were transfected with si–NGL-2, si-vec (empty vector) or si–NGL-2 + NGL-2* (siRNA-resistant NGL-2), with pEGFP-C1 (DIV 14–17). EGFP is shown in blue for better visualization. Scale bar, 10 µm. $n = 18$–24. $^*P < 0.001$ (Student's *t*-test). (**e**–**g**) NGL-2 knockdown did not affect VGAT-positive gephyrin clusters. Scale bar, 10 µm. $n = 12$. $P = 0.26$. (**h**–**j**) NGL-2 knockdown reduced the frequency (**i**), but not amplitude (**j**), of mEPSCs. $n = 31$–32. $^*P < 0.005$. (**k**–**m**) NGL-2 knockdown did not affect the frequency (**l**) or amplitude (**m**) of mIPSCs. $n = 13$–17. $P = 0.91$. Data represent mean ± s.e.m.

Unlike other isoforms in the neuroligin family, neuroligin 2 distributes to and promotes the differentiation of inhibitory synapses[16,17,21,30]. Our pan-NGL antibody did not detect any signals at inhibitory synapses, at least in immunohistochemical experiments, implying that the NGL family is unlikely to be involved in the differentiation of inhibitory synapses.

Like neurexin[13,24,25], both *netrin-G1* and *netrin-G2* exhibit extensive alternative splicing; at least ten different splice variants of *netrin-G1* have been identified[33–35,40]. In addition, the splicing pattern of *netrin-G1* differs in fetal and adult brains[40]. Therefore, the netrin-G–NGL adhesion might be regulated by alternative splicing of netrin-G, as shown in the neurexin-neuroligin adhesion[13,24–26,28]. In contrast to netrin-G, NGL does not exhibit extensive alternative splicing; instead, it contains a limited number of exons in coding regions (one for *NGL-1* and *NGL-2*, two for *NGL-3*). This suggests that NGL function may not be regulated by alternative splicing.

Role of the interaction between NGL and PSD-95

A previous report showed that surface-coated NGL-1 stimulates, but soluble NGL-1 disrupts, the outgrowth of developing thalamic neurons[36], suggesting that NGL-1 multimerization is important for netrin-G1 stimulation, just as neuroligin dimerization is important for presynaptic induction[15,41]. Although the possibility of NGL multimerization remains to be studied, PSD-95, which forms multimers through its N-terminal cysteines[42,43], may contribute to NGL multimerization.

NGL-2 overexpression increases the number of PSD-95–positive dendritic protrusions, and direct NGL-2 aggregation on the dendritic surface clusters PSD-95 and PSD-95–associated proteins. These results suggest that PSD-95 may couple the netrin-G–NGL adhesion with the recruitment of PSD-95–associated postsynaptic proteins for excitatory synaptic differentiation.

The fact that both neuroligin and NGL are directly linked to PSD-95 suggests that PSD-95 is a key postsynaptic scaffold linking trans-synaptic adhesion events to postsynaptic differentiation. A notable difference between NGL and neuroligin is that NGL binds to the first two PDZ domains of PSD-95, whereas neuroligin binds the third PDZ domain[14]. Therefore it is unlikely that NGL and neuroligin compete for binding; instead, they may collectively or synergistically determine the specificity of excitatory synaptic adhesion.

PSD-95 promotes excitatory synaptic localization of neuroligin 1 (ref. 31) and redirects neuroligin 2 from inhibitory to excitatory synapses[17,21], suggesting that the stoichiometry of PSD-95 and neuroligin isoforms may determine overall neuronal excitability[5]. Our data indicate that NGL-2 and PSD-95 are interdependent for excitatory synaptic localization. Therefore, NGL may participate in regulating the balance between excitation and inhibition in neurons.

Our data indicate that NGL-2 ΔC lacking PSD-95 binding promotes the formation of PSD-95–negative dendritic protrusions. This is reminiscent of the previous finding that neuroligin 1 ΔC lacking PSD-95 binding induces synaptic NMDA receptor recruitment[16], and suggests that both NGL and neuroligin

promote postsynaptic differentiation through PSD-95–dependent and PSD-95–independent mechanisms.

Clinical implications of the netrin-G–NGL interaction

Mutations in neuroligin 3 and neuroligin 4 have been directly associated with mental retardation and autism in human patients[44–46]. Some of the autism-related mutations decrease surface expression[47,48], but not synaptogenic activity[49], of the mutant proteins. Of note, a recent study of single nucleotide polymorphisms identified the association of netrin-G1 and netrin-G2 with schizophrenia[50]. In addition, the expression levels of mRNAs of some *netrin-G1* splice variants is markedly reduced in the brains of schizophrenic individuals[50]. These results implicate disturbances in netrin-G and NGL family proteins in clinically important brain dysfunctions.

METHODS

DNA constructs. Full-length mouse NGL-2 (DQ177325, aa 1–652; from a brain cDNA library; Clontech) and NGL-2 ΔC (1–649) were subcloned into pEGFP-N1. For bead aggregation, an Myc epitope (EQKLISEEDL) or EGFP was inserted between residues 46 and 47 of NGL-1, residues 44 and 45 of NGL-2, and residues 58 and 59 of NGL-3. For short-interfering RNA (siRNA) knockdown, nt 1488–1506 of rat NGL-2 (GATATCACCTGAGGACATA; DQ119102) were subcloned into pSilencer (Ambion). The siRNA-resistant NGL-2 expression construct contained two point mutations (A1494G and T1497C; no aa change). An Myc epitope was inserted between residues 43 and 44 of human netrin-G1c (BC030220) and between residues 32 and 33 of mouse netrin-G2a (AB052336).

Antibodies. Rabbit polyclonal pan-NGL (1,583) and NGL-2 specific (1,765) antibodies were raised using CIIQTHTKDKVQETQI (last 15 residues) and CTEISPEDITRKYKPV (aa 461–475 peptides, respectively). Other antibodies were purchased (**Supplementary Methods** online).

Immunoelectron microscopy. Postembedding immunoelectron microscopy was performed as described[48]. NGL antibodies (1,583) were used at 1 μg ml^{-1}. For quantitative electron microscopy, we used two immunoreacted sections from each of two rats labeled with secondary antibody to rabbit Fab fragments coupled to 10 nm gold particles (British BioCell). Using a cooled CCD camera (Gatan), we acquired (at 31,000× magnification) 139 randomly selected digital images of asymmetric synapses that had clearly outlined synaptic membranes and were labeled with at least one gold particle within 100 nm of the postsynaptic membrane. Images were analyzed using Scion Image software v.4.0. The axodendritic and tangential positions of 209 gold particles lying within ± 150 nm of the outer leaflet of the postsynaptic membrane were collected for analysis using Excel, CricketGraph and Kaleidograph software packages.

Coculture assay. Coculture assays were performed essentially as described[17,18]. Briefly, HEK293T cells transfected with NGL-2 constructs (Myc–NGL-2, Myc–NGL-2 ΔECD, or EGFP–NGL-2) or EGFP were cultured for 1–2 d, trypsinized, plated onto hippocampal neurons, cocultured for 3 d (DIV 9–12), and immunostained for Myc, synapsin I, EGFP or synaptotagmin (luminal domain). Vesicle turnover experiments were performed as described[38]. Briefly, neurons were incubated with synaptotagmin luminal domain antibodies (1:10 dilution) in isotonic depolarizing solution for 5 min.

Bead aggregation assay. Bead aggregation assays were performed as described[17]. For bead-induced presynaptic differentiation, neutravidin-conjugated FluoSphere beads (Molecular Probes; 1 μm diameter) were preincubated with biotin-conjugated antibodies to human and NGL-2-Ecto–Fc. Netrin-G2–expressing or untransfected cultured hippocampal neurons (DIV 9–12) were incubated with the beads for 24 h. For direct aggregation of NGL-2, beads preincubated with biotin-conjugated EGFP antibodies (Rockland) were added to cultured neurons expressing EGFP–NGL-2 (DIV 14–16) for 24 h before immunostaining.

Competition with soluble NGL-2. The ectodomain of NGL-2 (aa 1–483) was fused to the Fc region of human immunoglobulin (NGL-2-Ecto–Fc). Neurons transfected with pEGFP-C1 (for visualization of dendritic protrusions; DIV 12–14) were treated with NGL-2-Ecto–Fc for 3 d (10 μg ml^{-1}, refreshed daily).

Image acquisition and quantification. Images captured by confocal microscopy (LSM510, Zeiss) were analyzed in a blind manner using MetaMorph software (Universal Imaging). The density of dendritic protrusions (0.3–3.0 μm with or without head) and synaptic protein clusters was measured from 20–50 neurons; the total dendritic length of ~100 μm from the first dendritic branching points was measured for each neuron. Means from multiple individual neurons were averaged to obtain a population mean and s.e.m. For quantitation of synapsin I and synaptotagmin (luminal) clusters in the coculture assay, HEK293T cells were randomly chosen for image acquisition. Captured images were thresholded, and the integrated intensity of the clusters on a transfected HEK293T cell was normalized to the cell area.

Electrophysiology. Hippocampal cultured neurons were transfected with pSilencer NGL-2 or pSilencer and pEGFP-C1 at DIV 14. After 3 d, GFP-expressing neurons were whole-cell voltage-clamped at –70 mV using an Axopatch 200B amplifier (Axon instruments). Synaptic currents (mEPSCs and mIPSCs) were analyzed using Mini Analysis Program (Synaptosoft).

Note: Supplementary information is available on the Nature Neuroscience website.

ACKNOWLEDGMENTS

This work was supported by the National Creative Research Initiative Program of the Korean Ministry of Science and Technology (E.K.), and by grants from the Korea Science and Engineering Foundation (M10500000049-05J0000-04900 to H.K.) and the US National Institutes of Health (NS-39444 to R.J.W.).

AUTHOR CONTRIBUTIONS

A.B. and R.J.W. performed the light and electron microscopic studies. H.S.C. and H.K. conducted the *in situ* hybridization analysis. S.-K.K. performed the *in vivo* coimmunoprecipitation. J.W. did the coclustering assay. H.W.L. and K.K. performed the northern blot analysis.

COMPETING INTERESTS STATEMENT

The authors declare that they have no competing financial interests.

Published online at http://www.nature.com/natureneuroscience
Reprints and permissions information is available online at http://npg.nature.com/reprintsandpermissions/

1. Li, Z. & Sheng, M. Some assembly required: the development of neuronal synapses. *Nat. Rev. Mol. Cell Biol.* **4**, 833–841 (2003).
2. Waites, C.L., Craig, A.M. & Garner, C.C. Mechanisms of vertebrate synaptogenesis. *Annu. Rev. Neurosci.* **28**, 251–274 (2005).
3. Washbourne, P. *et al.* Cell adhesion molecules in synapse formation. *J. Neurosci.* **24**, 9244–9249 (2004).
4. Yamagata, M., Sanes, J.R. & Weiner, J.A. Synaptic adhesion molecules. *Curr. Opin. Cell Biol.* **15**, 621–632 (2003).
5. Levinson, J.N. & El-Husseini, A. Building excitatory and inhibitory synapses: balancing neuroligin partnerships. *Neuron* **48**, 171–174 (2005).
6. Craig, A.M., Graf, E.R. & Linhoff, M.W. How to build a central synapse: clues from cell culture. *Trends Neurosci.* **29**, 8–20 (2006).
7. Dean, C. & Dresbach, T. Neuroligins and neurexins: linking cell adhesion, synapse formation and cognitive function. *Trends Neurosci.* **29**, 21–29 (2006).
8. Akins, M.R. & Biederer, T. Cell-cell interactions in synaptogenesis. *Curr. Opin. Neurobiol.* **16**, 83–89 (2006).
9. Biederer, T. *et al.* SynCAM, a synaptic adhesion molecule that drives synapse assembly. *Science* **297**, 1525–1531 (2002).
10. Yamagata, M., Weiner, J.A. & Sanes, J.R. Sidekicks: synaptic adhesion molecules that promote lamina-specific connectivity in the retina. *Cell* **110**, 649–660 (2002).
11. Ichtchenko, K. *et al.* Neuroligin 1: a splice site-specific ligand for beta-neurexins. *Cell* **81**, 435–443 (1995).
12. Wu, Q. & Maniatis, T. A striking organization of a large family of human neural cadherin-like cell adhesion genes. *Cell* **97**, 779–790 (1999).
13. Ichtchenko, K., Nguyen, T. & Sudhof, T.C. Structures, alternative splicing, and neurexin binding of multiple neuroligins. *J. Biol. Chem.* **271**, 2676–2682 (1996).
14. Irie, M. *et al.* Binding of neuroligins to PSD-95. *Science* **277**, 1511–1515 (1997).
15. Dean, C. *et al.* Neurexin mediates the assembly of presynaptic terminals. *Nat. Neurosci.* **6**, 708–716 (2003).
16. Chih, B., Engelman, H. & Scheiffele, P. Control of excitatory and inhibitory synapse formation by neuroligins. *Science* **307**, 1324–1328 (2005).

17. Graf, E.R., Zhang, X., Jin, S.X., Linhoff, M.W. & Craig, A.M. Neurexins induce differentiation of GABA and glutamate postsynaptic specializations via neuroligins. *Cell* **119**, 1013–1026 (2004).
18. Scheiffele, P., Fan, J., Choih, J., Fetter, R. & Serafini, T. Neuroligin expressed in nonneuronal cells triggers presynaptic development in contacting axons. *Cell* **101**, 657–669 (2000).
19. Nam, C.I. & Chen, L. Postsynaptic assembly induced by neurexin-neuroligin interaction and neurotransmitter. *Proc. Natl. Acad. Sci. USA* **102**, 6137–6142 (2005).
20. Fu, Z., Washbourne, P., Ortinski, P. & Vicini, S. Functional excitatory synapses in HEK293 cells expressing neuroligin and glutamate receptors. *J. Neurophysiol.* **90**, 3950–3957 (2003).
21. Levinson, J.N. *et al.* Neuroligins mediate excitatory and inhibitory synapse formation: involvement of PSD-95 and neurexin-1beta in neuroligin-induced synaptic specificity. *J. Biol. Chem.* **280**, 17312–17319 (2005).
22. Hata, Y., Butz, S. & Sudhof, T.C. CASK: a novel dlg/PSD95 homolog with an N-terminal calmodulin-dependent protein kinase domain identified by interaction with neurexins. *J. Neurosci.* **16**, 2488–2494 (1996).
23. Biederer, T. & Sudhof, T.C. Mints as adaptors. Direct binding to neurexins and recruitment of munc18. *J. Biol. Chem.* **275**, 39803–39806 (2000).
24. Boucard, A.A., Chubykin, A.A., Comoletti, D., Taylor, P. & Sudhof, T.C. A splice code for trans-synaptic cell adhesion mediated by binding of neuroligin 1 to alpha- and beta-neurexins. *Neuron* **48**, 229–236 (2005).
25. Tabuchi, K. & Sudhof, T.C. Structure and evolution of neurexin genes: insight into the mechanism of alternative splicing. *Genomics* **79**, 849–859 (2002).
26. Rudenko, G., Nguyen, T., Chelliah, Y., Sudhof, T.C. & Deisenhofer, J. The structure of the ligand-binding domain of neurexin Ibeta: regulation of LNS domain function by alternative splicing. *Cell* **99**, 93–101 (1999).
27. Chih, B., Gollan, L. & Scheiffele, P. Alternative splicing controls selective trans-synaptic interactions of the neuroligin-neurexin complex. *Neuron* **51**, 171–178 (2006).
28. Graf, E.R., Kang, Y., Hauner, A.M. & Craig, A.M. Structure function and splice site analysis of the synaptogenic activity of the neurexin-1 beta LNS domain. *J. Neurosci.* **26**, 4256–4265 (2006).
29. Song, J.Y., Ichtchenko, K., Sudhof, T.C. & Brose, N. Neuroligin 1 is a postsynaptic cell-adhesion molecule of excitatory synapses. *Proc. Natl. Acad. Sci. USA* **96**, 1100–1105 (1999).
30. Varoqueaux, F., Jamain, S. & Brose, N. Neuroligin 2 is exclusively localized to inhibitory synapses. *Eur. J. Cell Biol.* **83**, 449–456 (2004).
31. Prange, O., Wong, T.P., Gerrow, K., Wang, Y.T. & El-Husseini, A. A balance between excitatory and inhibitory synapses is controlled by PSD-95 and neuroligin. *Proc. Natl. Acad. Sci. USA* **101**, 13915–13920 (2004).
32. Sara, Y. *et al.* Selective capability of SynCAM and neuroligin for functional synapse assembly. *J. Neurosci.* **25**, 260–270 (2005).
33. Nakashiba, T. *et al.* Netrin-G1: a novel glycosyl phosphatidylinositol-linked mammalian netrin that is functionally divergent from classical netrins. *J. Neurosci.* **20**, 6540–6550 (2000).
34. Nakashiba, T., Nishimura, S., Ikeda, T. & Itohara, S. Complementary expression and neurite outgrowth activity of netrin-G subfamily members. *Mech. Dev.* **111**, 47–60 (2002).
35. Yin, Y., Miner, J.H. & Sanes, J.R. Laminets: laminin- and netrin-related genes expressed in distinct neuronal subsets. *Mol. Cell. Neurosci.* **19**, 344–358 (2002).
36. Lin, J.C., Ho, W.H., Gurney, A. & Rosenthal, A. The netrin-G1 ligand NGL-1 promotes the outgrowth of thalamocortical axons. *Nat. Neurosci.* **6**, 1270–1276 (2003).
37. Valtschanoff, J.G. & Weinberg, R.J. Laminar organization of the NMDA receptor complex within the postsynaptic density. *J. Neurosci.* **21**, 1211–1217 (2001).
38. Kraszewski, K. *et al.* Synaptic vesicle dynamics in living cultured hippocampal neurons visualized with CY3-conjugated antibodies directed against the lumenal domain of synaptotagmin. *J. Neurosci.* **15**, 4328–4342 (1995).
39. Horejsi, V. *et al.* GPI-microdomains: a role in signalling via immunoreceptors. *Immunol. Today* **20**, 356–361 (1999).
40. Meerabux, J.M. *et al.* Human netrin-G1 isoforms show evidence of differential expression. *Genomics* **86**, 112–116 (2005).
41. Comoletti, D. *et al.* Characterization of the interaction of a recombinant soluble neuroligin-1 with neurexin-1beta. *J. Biol. Chem.* **278**, 50497–50505 (2003).
42. Hsueh, Y.P. & Sheng, M. Requirement of N-terminal cysteines of PSD-95 for PSD-95 multimerization and ternary complex formation, but not for binding to potassium channel Kv1.4. *J. Biol. Chem.* **274**, 532–536 (1999).
43. Christopherson, K.S. *et al.* Lipid- and protein-mediated multimerization of PSD-95: implications for receptor clustering and assembly of synaptic protein networks. *J. Cell Sci.* **116**, 3213–3219 (2003).
44. Jamain, S. *et al.* Mutations of the X-linked genes encoding neuroligins NLGN3 and NLGN4 are associated with autism. *Nat. Genet.* **34**, 27–29 (2003).
45. Laumonnier, F. *et al.* X-linked mental retardation and autism are associated with a mutation in the NLGN4 gene, a member of the neuroligin family. *Am. J. Hum. Genet.* **74**, 552–557 (2004).
46. Yan, J. *et al.* Analysis of the neuroligin 3 and 4 genes in autism and other neuro-psychiatric patients. *Mol. Psychiatry* **10**, 329–332 (2005).
47. Chih, B., Afridi, S.K., Clark, L. & Scheiffele, P. Disorder-associated mutations lead to functional inactivation of neuroligins. *Hum. Mol. Genet.* **13**, 1471–1477 (2004).
48. Comoletti, D. *et al.* The Arg451Cys-neuroligin-3 mutation associated with autism reveals a defect in protein processing. *J. Neurosci.* **24**, 4889–4893 (2004).
49. Chubykin, A.A. *et al.* Dissection of synapse induction by neuroligins: effect of a neuroligin mutation associated with autism. *J. Biol. Chem.* **280**, 22365–22374 (2005).
50. Aoki-Suzuki, M. *et al.* A family-based association study and gene expression nalyses of netrin-G1 and -G2 genes in schizophrenia. *Biol. Psychiatry* **57**, 382–393 (2005).